Morphological Method for Surface Metrology and Dimensional Metrology Based on Alpha Shape

Xiangqian Jiang*, Shan Lou, Paul J. Scott

EPSRC Centre for Innovative Manufacturing in Advanced Metrology, University of Huddersfield, Queensgate, Huddersfield, HD1 3DH, UK

E-mail: x.jiang@hud.ac.uk

Abstract. Morphological filters are useful tools as they are commonly employed in surface metrology and dimensional metrology, serving for surface texture analysis and data smoothing respectively. Compared to the mean-line filtering techniques, such as the Gaussian filter, morphological filters have the merits of compact support, no need to remove form, and being relevant to geometrical properties of surfaces. This paper proposes a novel morphological method based on the alpha shape. The proposed method has the advantages over the traditional methods that it runs relative fast, enables arbitrary large ball radii, and applies to freeform surfaces and nonuniform sampled surfaces. The theory of basic morphological operations and the alpha shape are introduced and the theoretical link between the alpha hull and the morphological closing and opening operation is presented. A practical algorithm is developed that corrects possible singularities caused by data spikes and reduces the amount of calculation for open profiles/surfaces. Computer simulation is used to compare the results from the traditional algorithm and the proposed one. Experimental studies are conducted to demonstrate the feasibility and applicability of using the proposed method.

1. Introduction

Surface metrology and dimensional metrology have profound influences on product manufacturing. Surface metrology inspects small scale geometrical features on product surfaces while dimensional metrology measures form and size in relative large scale. They work in a complementary manner to ensure the good quality and a satisfactory performance.

Filtration is a technique that separates the desirable features from other features in the data set. It is commonly used in surface metrology and dimensional metrology. In dimensional metrology, filtration plays a role of data smoothing while in surface metrology it usually serves as part of the analysis of the surface topography. Conventionally, there are two filtering systems: M-system (Mean-line filtering system) and E-system (Envelope filtering system). The mean-line filtering techniques decompose the surface signal into differing components according to their bandwidth in the frequency domain and thus extract the components of interest within the given wavelength bandwidth. The envelope filtering system is an alternative method depending on the geometrical structures of surfaces. The envelope filtration is achieved by rolling a ball of the selected radius over the surface (Von Weingraber 1956).

The Gaussian filter, the most typical representative of the M-system techniques, is the standardized filter both for surface metrology and dimensional metrology (ISO 11562 1994). It is based on the time-frequency analysis technique, which convolves the signal with the weighting function (Gaussian function) to obtain the weighted average value. In surface metrology, the Gaussian filter is employed

to decompose the primary surface into different scale-limited surface components (If we take a traditional approach, it means to separate the primary surface into roughness and waviness components) (Whitehouse 1994). In dimensional metrology the Gaussian filter serves as a smoothing method for linear and roundness data. However, the Gaussian filter has several limitations. First, before filtering, the irrelevant form needs to be removed from the measured data to obtain the residual surface on which the Gaussian filter is performed. Otherwise the form will cause distortions. Second, the Gaussian filter is sensitive to outliers. Third, the Gaussian filter takes the pre-requisition that the residual surface can be broken down into a series of harmonic components.

The envelope filter, regarded as the complement to mean-line filters, has merits against the limitations mentioned above. It is relative to the geometrical properties of surfaces and thus gives better results on the functional prediction of surfaces. It has compact support, taking care of both amplitude and spatial information. Furthermore, it does not require the form to be removed. With the introduction of mathematical morphology, morphological filters emerged as the evolution of the envelope filtering system (Srinivasan 1998; Scott 2000). Morphological filters are essentially the superset of the early envelope filter, offering more tools and capabilities. They are carried out by performing morphological operations on the input signal (profile/surface) with the circular or flat structuring element, usually circular. Over the last decade, morphological filters have found many applications in practice. The morphological closing filter was utilized to approximate the conformable interface of two mating surfaces (Malburg 2003). The morphological alternating symmetrical filter was employed to decompose the surface topography of an internal combustion engine cylinder (Decenciere & Jeulin 2001). ISO 16610 (2010) illustrated an example of detecting the defective milling mark from a milled surface using the morphological scale-space technique.

Although morphological filters are useful and generally accepted, existing algorithms (Shunmugan & Radhakrishnan 1974; ISO 16610 2010; Scott 1992) have some drawbacks. For one thing, these methods are either time-consuming, especially for large data set and large structuring element, or hard to extend to areal data. Further, the maximum ball radius is limited in practice due to the huge computational requirement, while for many real applications they may desire ball (disk) radii much larger than the signal length, particularly for surfaces with the form attached. What's more, these methods are restricted to "planar" surfaces, namely two-dimension manifolds embedded in the Euclidean spaces R^3 (Jiang et al. 2010). With the advancement of the modern manufacturing techniques, more complex surfaces emerge. These complex surfaces have no rotational or translational symmetry, and are referred to as freeform surfaces (Jiang et al. 2007). For freeform surfaces, the data might be specified by coordinate pairs/triplets rather than regular surface heights, thus these methods do not work.

In this paper, we propose a novel morphological method which is based on the alpha shape. The alpha hull is theoretically linked to the morphological operations. It provides a feasible tool to compute morphological filters. The proposed method works for both profile and areal data with relative fast speed over the traditional methods for area data. Arbitrary large ball radii are available, bringing more applicability to morphological filtering. Another merit derived from the proposed method is that it applies to the freeform surfaces and the nonuniform sampled surfaces. The nomenclature used in this paper is given in the Table 1.

Table 1. Nomenclature.

$A \oplus B$	The dilation of A by B
$A \ominus B$	The erosion of A by B
$A \bullet B$	The closing of A by B
$\overset{\vee}{B}$	The reflection of B through the origin of B
$S \subset R^d$	Point set S in R^d
∂b	The boundary of b
S_α	The alpha shape of the point set S with the alpha ball radius α
σ_T	k-simplex where $\lvert T \rvert = k+1$
$DT(S)$	Delaunay triangulation of the point set S
$C_\alpha(S)$	The alpha complex of the point set S with the alpha ball radius α
$\overset{\circ}{B}$	The interior of B
X^c	The complement of X
$H_\alpha(X)$	The alpha hull of X

2. Basic morphological operations

Mathematical morphology is a mathematical discipline established by two French researchers Jorge Matheron and Jean Serra in the early the 1960s (Serra 1982). The central idea of mathematical morphology is to examine the geometrical structure of an image by matching it with small patterns at various locations in the image. By varying the size and the shape of the matching patterns, called structuring elements, one can exact useful information about the shape of the different parts of the image and their interrelation (Heijmans 1995). There are four basic morphological operations, namely dilation, erosion, opening and closing, which form the foundation of mathematical morphology.

2.1. Dilation and Erosion

Dilation combines two sets using the vector addition of set elements. The dilation of A by B is

$$D(A,B) = A \oplus \overset{\vee}{B}. \tag{2.1}$$

It is defined on the basis of vector addition, also known as the Minkowski addition, which was first introduced by Minkowski (1903). The Minkowski addition of two input sets A and B is the set:

$$A \oplus B = \{c \mid c = a + b, a \subseteq A \ \& \ b \subseteq B\}. \tag{2.2}$$

Erosion is the morphological dual to dilation. It combines two sets using the vector subtraction of set elements. The erosion of A by B is

$$E(A,B) = A \ominus \overset{\vee}{B}, \tag{2.3}$$

where

$$A \ominus B = \left(A^c + B\right)^c. \tag{2.4}$$

Dilation and erosion are two elementary operations of mathematical morphology. Dilation expands the input set by the structuring element, while erosion shrinks the input set by the structuring element. Figure 1 shows examples of the dilation and erosion of a square by a disk.

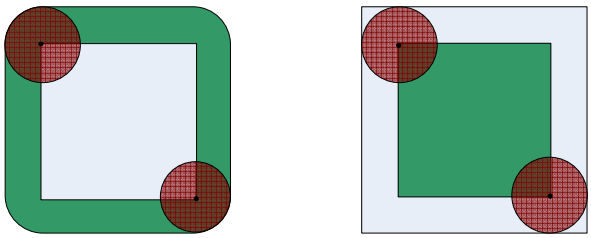

Figure 1. Dilation and erosion of a square by a disk. (a) The dilation of the light colour square by a disk results in the dark colour square with round corners. (b) The erosion of the light colour square by a disk generates the dark colour square.

2.2. Opening and Closing

Opening and closing are dilation and erosion combined pairs in sequence. The opening of A by B is obtained by applying the erosion followed by the dilation,

$$O(A,B) = D(E(A,B),\check{B}). \tag{2.5}$$

Closing is the morphological dual to opening. The closing of A by B is given by applying the dilation followed by the erosion,

$$C(A,B) = E(D(A,B),\check{B}). \tag{2.6}$$

Opening and closing are two secondary operations of mathematical morphology. The result of applying opening and closing is an elimination of specific features whose size are smaller than the structuring element. Figure 2 shows examples of the opening and closing of a square(s) by a disk.

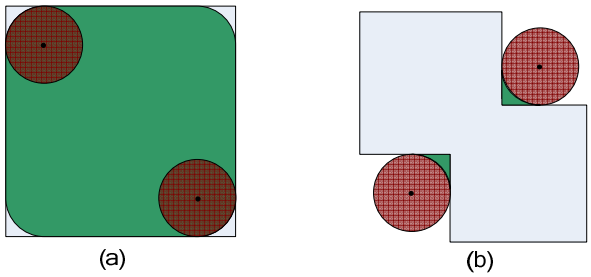

Figure 2. Opening and closing of a square(s) by a disk. (a) The opening of the light colour square by a disk generates the dark colour square with round corners. (b) The closing of the light colour shape (union of two squares) by a disk results in the union of the light colour shape and the dark colour areas.

3. Alpha shape for shape description

The alpha shape was introduced by Edelsbrunner in the 1980's aiming to describe the specific "shape" of a finite point set with a real parameter controlling the desired level of details (Edelsbrunner & Muche 1994). Conceptually the alpha shape is a generalization of the convex hull of a point set. Imagine a huge block of styrofoam making up the space containing some solid particles. To use a spherical eraser of radius α to carve out all the styrofoam blocks from inside and outside without bumping into the solid particles (See figure 3), it will eventually end up with an object with arcs, caps and points. The boundary of the resulting object is called the alpha hull. If the round faces of the

object are straightened by line segments for arcs and triangles for caps, another geometrical structure, the alpha shape, forms (Fischer 2000).

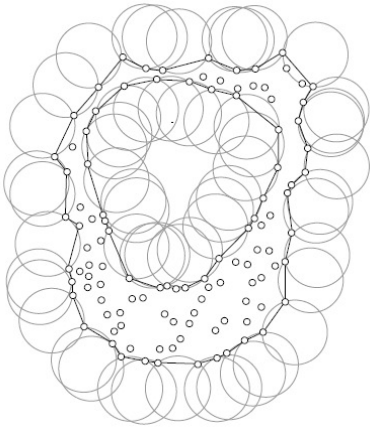

Figure 3. Alpha hull and alpha shape of planar points (Fischer 2000).

3.1. Alpha shape

In the context of the alpha shape, the sphere eraser in the above example is called the alpha ball. It is formally defined as an open ball of radius α. Given a point set $S \subset R^d$, a certain alpha ball b is empty if $b \bigcap S = \varnothing$. With this, a *k*-simplex σ_T ($|T| = k+1$) is said to be α-exposed if there exists an empty alpha ball b with $T = \partial b \bigcap S$ where ∂b is the surface of the sphere (for d=3) or the circle (for d=2) bounding b, respectively.

For $0 \le \alpha \le \infty$, the alpha shape of S, denoted by S_α, is defined as the complement of the union of all empty α-balls. ∂S_α, the boundary of the alpha shape of the point set S, consists of all *k*-simplexes of S for $0 \le k < d$ which are α-exposed,

$$\partial S_\alpha = \{\sigma_T \mid T \subset S, |T| = k+1, \sigma_T \ \alpha - exposed\} \tag{3.1}$$

3.2. Delaunay triangulation and alpha complex

The computation of the alpha shape is based on the Delaunay triangulation which is one of the most exhaustively examined problems in computational geometry (O'Rourke 1994). Given a point set $S \subset R^d$, the Delaunay triangulation is a triangulation $DT(S)$ such that no point in S is inside the circumsphere of any *d*-simplexes σ_T with $T \subset S$. The relationship between the Delaunay triangulation and the alpha shape is that the boundary of the alpha shape ∂S_α is a subset of the Delaunay triangulation of S, namely

$$\partial S_\alpha \subset DT(S). \tag{3.2}$$

3.3. Alpha complex

The relationship (3.2) means all the simplexes in $DT(S)$ are candidates for the alpha shape. In order to further find which simplex in $DT(S)$ belongs to ∂S_α, another concept, alpha complex $C_\alpha(S)$, was introduced.

Set ρ_T the radius of the smallest circumsphere b_T of σ_T. For $k = 3$, b_T is the circumsphere; For $k = 2$, b_T is the great circle; And for $k = 1$, the two points in T are antipodal on b_T.

For a given point set $S \subset R^d$, the alpha complex $C_\alpha(S)$ of S is the following simplicial subcomplex of $DT(S)$. A simplex $\sigma_T \in DT(S)$ ($|T| = k+1,\ 0 \le k \le d$) is in $C_\alpha(S)$ if:

- $\rho_T < \alpha$ and ρ_T-ball is empty, or
- σ_T is a face of other simplex in $C_\alpha(S)$.

The link between the alpha complex and the alpha shape is: the boundary of the alpha complex makes up the boundary of the alpha shape, i.e.

$$\partial C_\alpha(S) = \partial S_\alpha(S) \in DT(S). \tag{3.3}$$

4. Link between the alpha hull and morphological operations

The boundary of the alpha hull is obtained by rolling the alpha ball over the point set. By intuition the alpha hull seems very similar to the secondary morphological operations, opening and closing, as the alpha ball acts as a circular structuring element and the input set as the points set. In fact a theoretical link exists between the alpha hull and morphological opening and closing, as proved by Worring and Smedulers (1994). They extended Edelsbrunner's work, proposed the alpha graph and utilized it to describe the boundary of the point set. They also found the relationship between the alpha graph and the opening scale space from mathematical morphology, which is given by equation (4.1):

$$\begin{aligned} S_\alpha(X) &= \left(\left(X \oplus \mathring{B}_{-\alpha} \right)^c \oplus \mathring{B}_{-\alpha} \right)^c \\ &= \left(X \oplus \mathring{B}_{-\alpha} \right) \ominus \mathring{B}_{-\alpha} \\ &= X \bullet \mathring{B}_{-\alpha} \end{aligned} \quad . \tag{4.1}$$

Equation (4.1) proves that the alpha hull is equivalent to the closing of X with a generalized ball of radius $-1/\alpha$. Hence from the duality of the closing and the opening, the alpha hull is the complement of the opening of X^c with the same ball as the structuring element.

5. Proposed algorithm based on alpha shape

In surface metrology and dimensional metrology, surfaces are measured by measurement instruments. The measured points are a discrete representation of the surface. Viewing this sampled data as a finite point set in the context of the alpha shape and according to the link between the alpha hull and morphological operations, we employ the alpha shape to compute morphological filters for surfaces.

5.1. Spike detection and points interpolation

In practical measurement of surfaces, it may happen that sharp spikes exist in sample data. Sometimes the space between the peak point and the pit point is quite large that the ball will run into the interior of the profile/surface. This is not allowed in reality because the real surface is physically continuous and won't allow the ball to enter. The difference between the physical continuity of the surface and the discrete representation of the sample data is the quintessence of this problem.

To correct these singularities, sharp spikes should be detected and enough points linearly interpolated on the ridge of the spike to prevent the ball from passing through. The whole process is elaborately depicted in figure 4 for the case of profile data. For areal data, surfaces can degenerate to profiles if considering them as the composition of parallel profile sections. There is a trivial difference between the closing envelope and the opening envelope in their spike detection. For the closing envelope, it suffices to detect peak spikes in that the closing envelope is only determined by peaks, and valleys could be ignored. As opposed it is enough to search valleys for the opening envelope because the opening envelope is only affected by valleys.

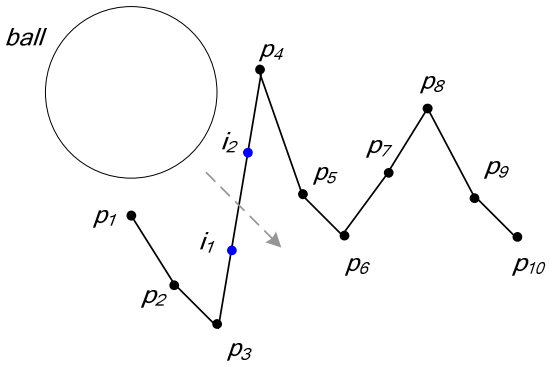

Figure 4. Spikes detection in measured data following by linear interpolation of points. p_1, p_2, …, p_{10} are the sample points on the original profile. $p_3 p_4 p_5$ forms a local peak. p_3 and p_4 are spacing far from each other that the ball could roll into the profile interior. In this case the additional points i_1, i_2 (and more if needed) are linearly interpolated to reduce the gap between p_3 and p_4.

5.2. Alpha shape computation

With the justified data, the next step of the computation is to triangulate the data set by the Delaunay triangulation and subsequently obtain the facets of the boundary of the alpha shape, which are also contained in the boundary of the alpha complex ∂C_α according to the section 3.

Delaunay triangulation results in a series of *k*-simplexes σ ($k = 2$ for profiles, which are triangles, and $k = 3$ for surfaces, which are tetrahedrons). These k-simplexes can be categorized into two groups: k-simplexes σ_p whose circumsphere radius is larger than the radius of the rolling ball α, and k-simplexes σ_{np} whose is no larger than α.

σ_p consists of two parts: the $(k-1)$-simplexes σ_{int} interior to σ_p, and the $(k-1)$-simplexes σ_{reg} that bounds its super k-simplexes σ_p. We called σ_{reg} the regular facets. σ_{np} is comprised of three components: the $(k-1)$-simplexes σ_{ext} out to C_α, part of the regular facets σ'_{reg} shared by both σ_p and σ_{np}, and the $(k-1)$-simplexes σ_{sing} that is the other part of ∂C_α. We call σ_{sing} the singular facets. σ_{sing} differs from σ_{reg} in that it does not bound any super k-simplexes. σ_{sing} satisfies two conditions as follows:

- The radius of its smallest circumsphere is smaller than α.
- The smallest circumsphere is empty.

The regular facets σ_{reg} and the singular facets σ_{sing} form the whole boundary of the alpha complex, i.e. the boundary of the alpha shape, as the equation (5.1) presents.

$$\partial S_\alpha = \partial C_\alpha = \sigma_{reg} + \sigma_{sing} \tag{5.1}$$

```
Procedure AlphaShape (S, α)
{Given a justified data set S and the chosen ball radius α, computes}
{two lists σ_reg, σ_sing of the regular facets and the singular facets }
{of the boundary of the alpha shape of S.}
Begin
    σ_{k+1} =DelaunayTri(S);
    i=1; j=1;
    for each σ_k do
        r=CircumSphere(σ_{k+1});
        if r<α
            if Unique(σ_k)
                σ_reg(i)= σ_k;
                i=i+1;
            end if;
            continue;
        end if;
        r=SmallCircumSphere(σ_k);
        if r<α
            if IsSphereEmpty(σ_k)
                σ_sing(j)= σ_k;
                j=j+1;
            continue;
            end if;
        end if;
    end for;
    return (σ_reg, σ_sing);
end AlphaShapes;
```

Figure 5. Skeleton of the algorithm to compute the facets of the boundary of the alpha shape. The *DelaunayTri* operation generates a list of *k*-simplex σ_{k+1} (*k=2* for profile data and *k=3* for areal data). The algorithm loops to check if each (*k-1*)-simplex σ_k is the regular facet σ_{reg} or the singular facet σ_{sing}. The *CircumSphere* operation computes the radius of the circumsphere of σ_{k+1}. *SmallCircumSphere* operation calculates the radius of the smallest circumsphere of σ_k. The *Unique* operation checks if σ_k's super simplexes σ_{k+1} with their circumsphere radius larger than α are unique. The *IsSphereEmpty* operation detects if the circumsphere of σ_k is empty.

The skeleton of the algorithm for computing the regular facets and the singular facets of ∂S_α is given by figure 5. The algorithm integrates the search of the facets of ∂S_α in a loop and outputs the regular facets and the singular facets separately so that they could be handled respectively by later manipulations. Aiming to improve the algorithm efficiency, a useful property of the alpha shape is applied to speed up the *IsSphereEmpty* operation, i.e. empty ball testing. The property is to test whether the circumsphere of a facet is empty it suffices to check whether the opposite vertices of its super simplexes are out to the circumsphere boundary. It is much more efficient than checking all other points, which could be huge in the case of areal data. Figure 6 illustrates an example of the sample points of a surface along with the facets of ∂S_α. In fact, the vertices of these boundary facets are the points on the surface that contact the ball (disk) as it is rolling over the surface all around.

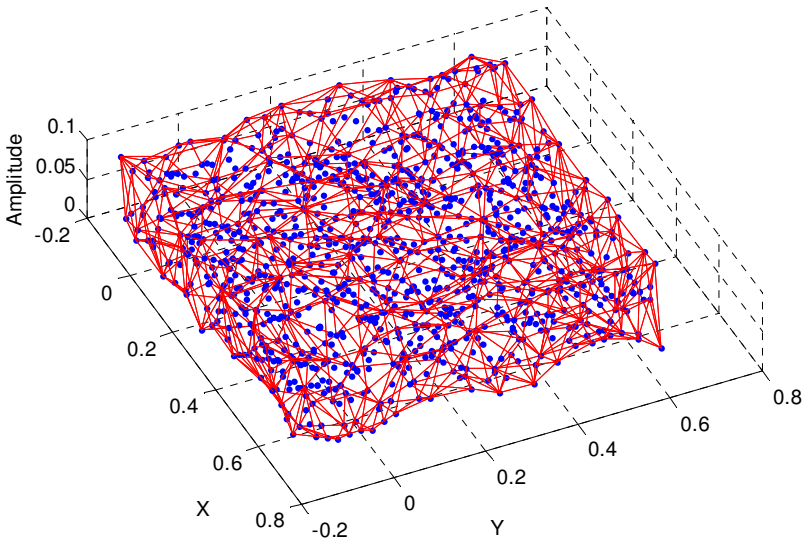

Figure 6. Areal sample points of a surface and the facets of the boundary of the alpha shape.

5.3. Facets reduction

Having the facets of ∂S_α, opening and closing envelopes could be calculated. For open profiles/surfaces, not all but part of the facets of ∂S_α is needed for the computation of a certain envelope. For closing envelopes, only the upper part of the regular facets is of interest, and vice versa for opening envelopes. Therefore the number of the regular facets used for the envelope computation could be reduced by extracting those facets which are possible candidates for the computation.

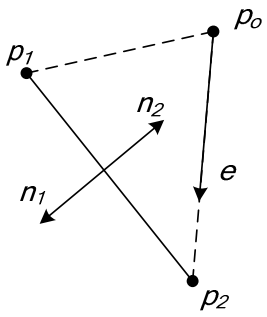

Figure 7. Determination of the normal of a regular facet. p_1p_2 is one of the regular facets. p_o is the opposite vertex of its super simplex $p_1p_2p_o$. The facet p_1p_2 has two possible normal vectors, n_1 pointing outward, and n_2 pointing inward. The vector e which is from p_o to one of the facet vertices (p_1 or p_2) determines the outward direction. Being consistent with the orientation of e, n_1 is chosen as the normal of the facet p_1p_2.

Regular facets can be separated according to their normals. We define the normal of a facet as the vector that is perpendicular to the facet and pointing from the interior of boundary shape to its outside. The regular facet has an unique super simplex. The opposite vertex in its super simplex could help to

justify the normal vector from two possible candidate perpendicular vectors. Figure 7 illustrates how a facet normal is achieved for profile data. This method could be also reasonably extended to areal data.

Once the normals of the regular facets are settled, the separation of the upper part and lower of regular facets is available. The regular facets are connected and their normals are oriented consistently. As to the upper part of the regular facets, their facet normals are oriented upward, and vice versa. Thus this property could be used to separate the upper part and lower part of the regular facets. Figure 8 demonstrates the separation of the upper regular facets and the lower regular facets. For the singular facets, this idea does not make sense for two reasons. On one hand, the singular facet may have more than one super simplex, therefore unable to determine its normal. On the other hand, even though a singular facet only has one super simplex, it is still hard to determine the normal because the singular facets could be disconnected and the vector e used in figure 7 cannot indicate the outward or inward orientation.

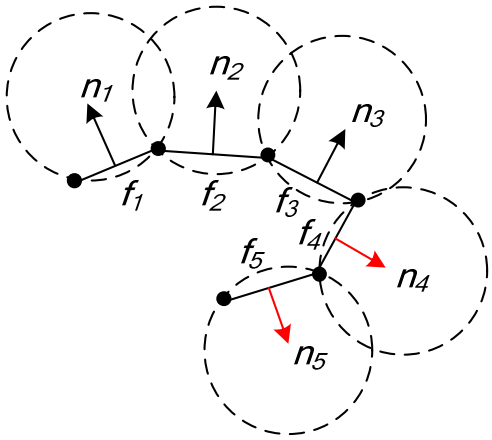

Figure 8. Separation of the upper regular facets and the lower regular facets. f_1, f_2, $\cdots$, f_5 are part of the regular facets of the boundary of the alpha shape, with n_1, n_2, $\cdots$, n_5 being their normals respectively. Suppose the ball are rolling from f_1 to f_5. The normal of first three facets n_1, n_2, n_3 are oriented consistently (all of them are pointing upward). Then the ball continues to roll to the facet f_4, the facet normal n_4 turns to orient downward, and n_5 keep consistent with n_4, orienting downward also. Hence the facets can be separated into two parts: f_1, f_2, f_3 are the upper facets, and f_4, f_5 are the lower facets. For the computation of the closing envelope, the lower facets f_4, f_5 are neglected because they have no impact on the computation of the closing envelope.

5.4. Envelope point calculation

The final step is the calculation of the envelope points. For each sample point, there is a one-to-one corresponding point on the envelope. These points form a discrete representation of the envelope. Each facet of the boundary of the alpha shape determines its counterpart on the alpha hull. Due to the fact that the target envelope is contained in the alpha hull, we project the sample points onto the alpha hull in the direction of the local gradient vector and record the extreme project coordinates, namely the envelope point for this sample point.

For "planar" open surfaces, all of the local gradient vectors are supposed to be perpendicular to the reference plane, i.e. the amplitude direction. Figure 9 illustrates the acquisition of the closing envelope points by projecting them onto the alpha hull for the planar open profile data (a) and areal data (b) respectively. We recorded the extreme projection heights for all the sample positions (Highest heights for the closing envelope and lowest heights for the opening envelope). These extreme projection coordinates are the final results for the target envelope.

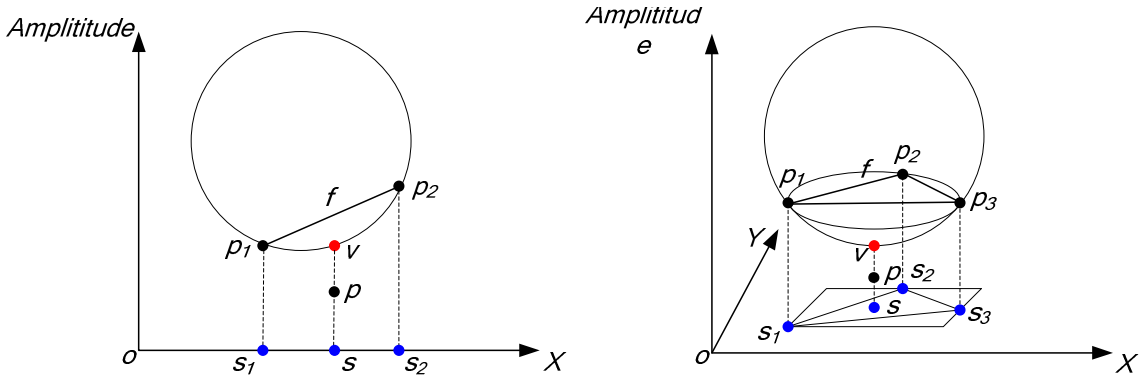

Figure 9. The acquisition of the closing envelope points by projecting onto the alpha hull for the planar open profile (a) and open surface (b). (a) The facet f determines an arc $\overset{\frown}{p_1p_2}$ from the point p_1 to p_2, which is a part of the alpha hull. The sample point p has its sampling position s between the sampling position s_1 and s_2 for p_1 and p_2 respectively. p is projected to the arc $\overset{\frown}{p_1p_2}$ in the amplitude direction to obtain the envelope point v. (b) The facet f determines a cap $\overset{\frown}{p_1p_2p_3}$ as a part of the alpha hull. The sample point p has it sampling position s inside the triangle area $\Delta s_1s_2s_3$. s_1, s_2 and s_3 are the sampling position for p_1, p_2 and p_3 respectively. p is projected to the cap $\overset{\frown}{p_1p_2p_3}$ in the direction of amplitude to obtain the envelope point v.

6. Computer simulation

For the purpose of verifying the proposed method, a surface with "noise" and 100×100 points was created aiming to compare the traditional algorithm (ISO 16610 2010) and the proposed one. See figure 10(a). The surface is 1×1 mm^2 in area with sampling interval 0.01 mm. The surface was filtered by the morphological closing filter with ball radius 0.15 mm. Figure 10(b) presents the closing envelope resulting from the traditional algorithm. By comparison, the resulting envelope computed by the alpha shape method is illustrated in figure 10(c). Figure 10(d) presents the comparison of two envelopes. The comparison reveals that the two results are basically in agreement except at the boundary region of the surface. This is caused by the end effect of filtration on the open surface data. The traditional algorithm has the end effect corrected while the proposed method does not. It remains a research issue for the future.

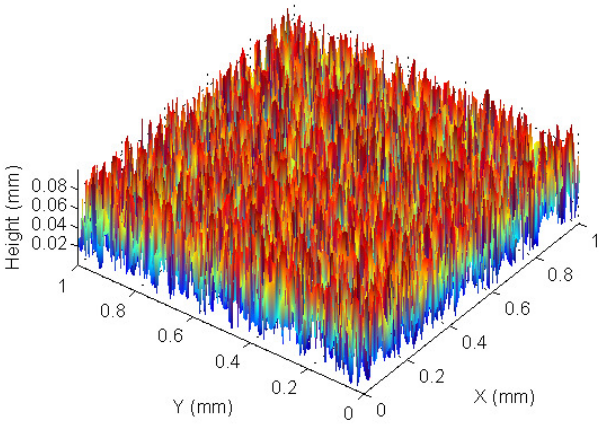
Height (mm)
0.08
0.06
0.04
0.02
1
0.8
0.6
0.4
0.2
0
Y (mm)
0
0.2
0.4
0.6
0.8
1
X (mm)

(a)

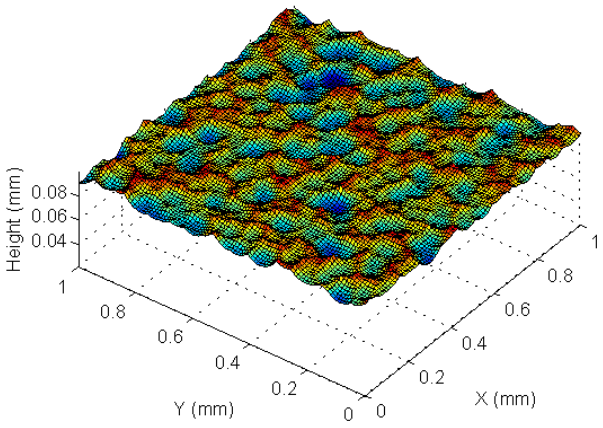
Height (mm)
0.08
0.06
0.04
1
0.8
0.6
0.4
0.2
0
Y (mm)
0
0.2
0.4
0.6
0.8
1
X (mm)

(b)

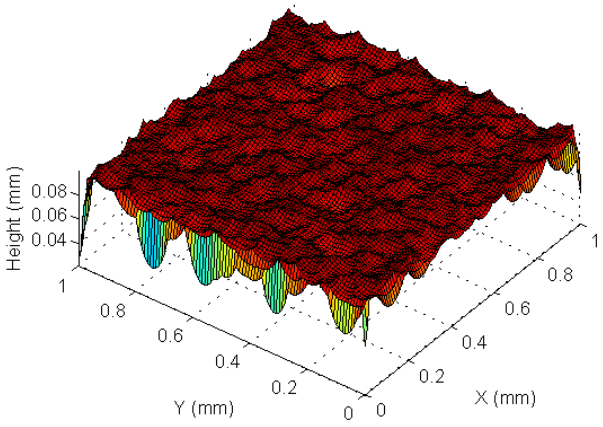
Height (mm)
0.08
0.06
0.04
1
0.8
0.6
0.4
0.2
0
Y (mm)
0
0.2
0.4
0.6
0.8
1
X (mm)

(c)

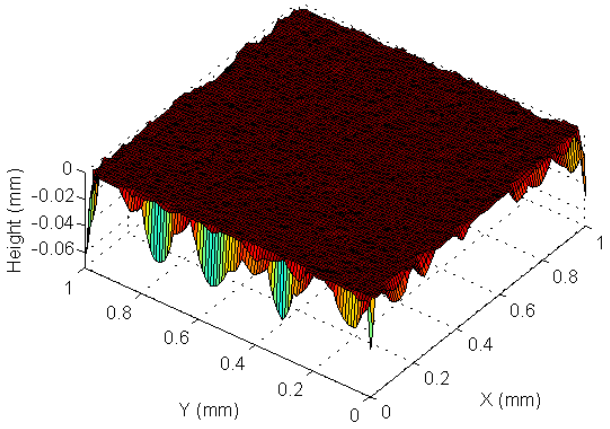

(d)

Figure 10. Simulation of applying the morphological closing filter by the traditional algorithm and the proposed algorithm respectively. (a) Raw surface. (b) Closing envelope computed by the traditional algorithm. (c) Closing envelope computed by the proposed algorithm. (d) Deviation between two resulting envelopes.

7. Experimental studies

Following the initial application of the proposed method to simulated data, the method was performed on real surface measurement data. The measurement data was acquired by Taylor Hobson PGI on a portion of a worn artificial knee replacement component. The data are composed of 236 × 236 points taken on an approximately square grid. The whole area is 181.72 × 155.76 μm^2 with the sampling interval 0.77 μm on the X direction and 0.66 μm on the Y direction. See figure 11(a). Figure 11(b) shows the resulting morphological closing envelope by a 5mm ball. The surface presented in figure 11(c) is the residual surface obtained by subtracting the envelope surface from the original surface. Wear marks are easy to detect on the residual surface, enabling further tribological analysis to the component.

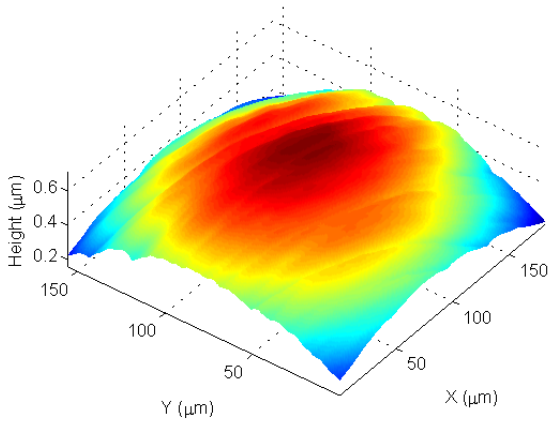

(a)

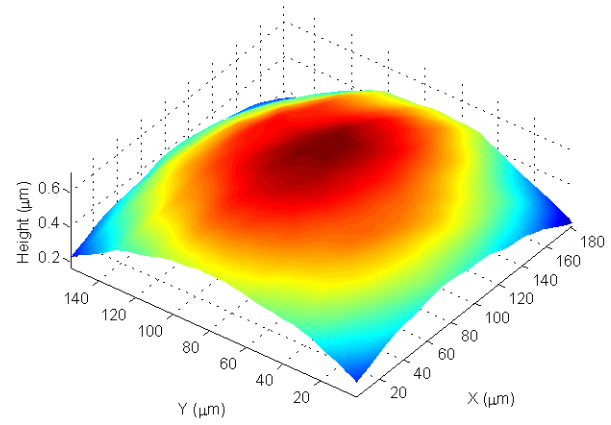

(b)

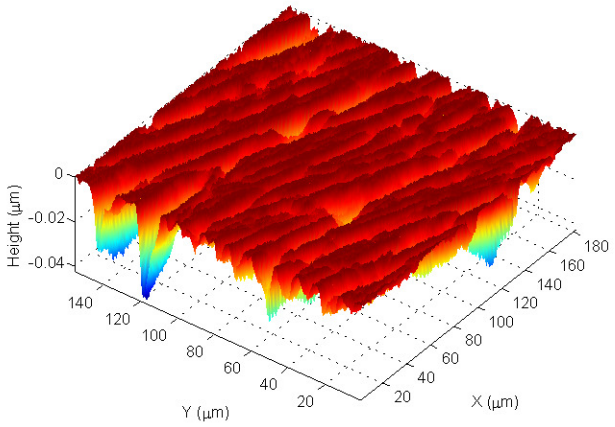

(c)

Figure 11. Applying the morphological closing filter on a portion of a worn artificial knee replacement component. (a) Original surface. (b) Morphological closing envelope surface. (c) Residual surface.

Another experiment was performed on a milled surface. The surface area is 5.11 x 5.11 μm^2 with 2962 sampling points. As marked by the dots in figure 12(a), these sampling points are nonuniform sampled on the surface. Then the morphological closing filter was performed on these nonuniform sampled points using the proposed approach with a 15 μm ball. The resulting envelope points are illustrated in figure 12(b), shown as the dots above the original surface.

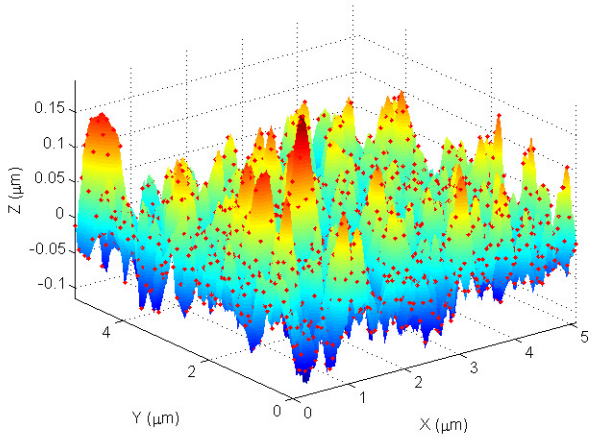

(a)

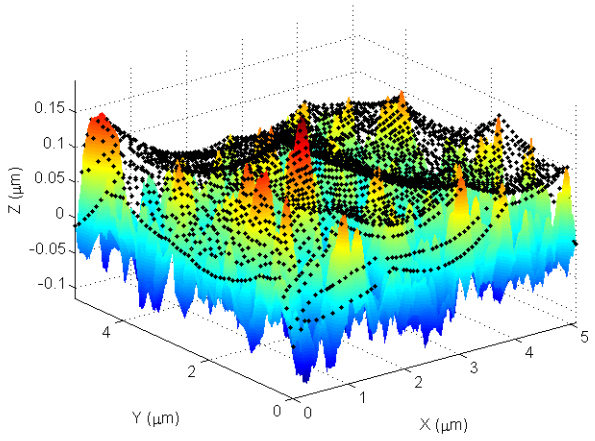

(b)

Figure 12. Morphological closing filter on the nonuniform sampled surface. (a) The original surface with the nonuniform sampled points. (b) The original surface with the closing envelope points.

8. Conclusion and future work

Morphological filters, evolved from the traditional envelope filtering system, play important roles in surface metrology and dimensional metrology as the complementary tool to the mean-lined filters. Aiming to solve the limitations of existing algorithms for morphological filters, we proposed a novel approach based on the alpha shape, providing the merits of running relative fast, arbitrary large ball radii available, freeform surfaces and nonuniform sampled surface applicable. The proposed approach utilizes the theoretical link between the alpha hull and the morphological closing and opening operation. A practical algorithm was developed with the attentions to correct possible singularities caused by data spikes and the efforts to reduce the amount of computation for open surfaces/profiles. The computer simulation was performed by applying the morphological closing filter to both the traditional algorithm and the proposed algorithm. It revealed that the two resulting envelopes are in agreement except at the boundary region of the surface. Two practical examples were presented, which use the proposed method to perform the morphological closing filtering on the free form surface of an industrial component and a nonuniform sampled surface respectively. They have initially demonstrated the feasibility and applicability of the alpha shape method.

A key area of the future research will be the correction of the end effect of this methodology. The end effects are common in the filtration of open profiles/surfaces, characterized by certain distortion within the scope of the cutoff wavelength or the ball radius around the boundary of the resulting data. An efficient correction method would be of interest. Another area of the future work will be the development of ways to speed up the algorithms. Although 3D Delaunay triangulation runs in $O(nlogn)$ time complexity which is relative faster than existing algorithms for morphological area filters and the triangulation data could be reused for multiple attempts on the same measured profile/surface, it is costly in computing time and memory in its initial generation, especially in the case of huge data sets of million points.

Acknowledgements

The author X. Jiang gratefully acknowledges the Royal Society under a Wolfson-Royal Society Research Merit Award. The authors gratefully acknowledge the European Research Council for its "Ideal Specific programme" ERC-2008-AdG 228117-Surfund and the UK research council for its "manufacturing the future" program on the EPSRC centre in advanced metrology.

References

Decenciere E and Jeulin D 2001 Morphological decomposition of the surface topography of an internal combustion engine cylinder to characterize wear *Wear* 249 482-488

Edelsbrunner H and Mucke E P 1994 Three-dimensional alpha shapes *ACM Trans. Graph.* 13(1) 43-72

Fischer K 2000 Introduction to Alpha Shapes *http://www.inf.ethz.ch/personal/fischerk/pubs/as.pdf*

Heijmans H J A M 1995 Mathematical morphology: a modern approach in image processing based on algebra and geometry *SIAM Review* 37 1-36

ISO 11562 1996 Geometrical Product Specification (GPS)–Surface texture: Profile method–Metrological characteristics of phase correct filter

ISO 16610 2010 Geometrical Product Specification (GPS)–Filtration

Jiang X, Scott P J, Whitehouse D J and Blunt L 2007 Paradigm shifts in surface metrology, Part II. The current shift *Proc. R. Soc. A*. 463(2085) 2071-2099

Jiang X, Copper, P and Scott P J 2011 Freeform surface filtering using the diffusion equation *Proc. R. Soc. A*. 467(2127) 841-859

Malburg C M 2003 Surface Profile Analysis for Conformable Interfaces *Transactions of ASME* 125 624-627

Minkowski H 1903 Volumen and oberflache *Matheatical Annals* 57 447-495

O'Rourke J 1994 *Computational geometry in C* New York: Cambridge University Press

Scott P J 1992 The mathematics of motif combination and their use for functional simulation *Int. J. Mach. Tools Manufact.* 32 69-73

Scott P J 2000 Scale-space techniques *Proceedings of the X International Colloquium on Surfaces* 153-161

Shunmugam M S and Radhakrishnan V 1974 Two-and three dimensional analyses of surfaces according to the E-system *Proc. Instn. Mech. Eng.* 188 691–699

Serra J 1982 *Image Analysis and Mathematical Morphology* Academic Press New York

Srinivasan V 1998 Discrete morphological filters for metrology *Proceedings 6th ISMQC Symposium on Metrology for Quality Control in Production*

Von Weingraber H 1956 Zur Definition der Oberflächenrauheit *Werkstattstechnik Masch. Bau.* 46

Whitehouse D J 1994 *Surface Metrology* Bristol and Philadelphia: Institute of physics publishing

Worring M and Smelders W M 1994 Shape of arbitrary finite point set in R2 *Journal of Mathematical Image and Vision* 4 151-170